Laurencena, B. R., and M. C. Williams, "Radial Flow of Non-Newtonian Fluids Between Parallel Plates," *Trans. Soc. Rheol.*, 18, 331 (1974).
Leider, P. J., "Squeezing Flow Between Parallel Disks" II. Experimental Results," *Ind. Eng. Chem. Fundamentals*, 13, 342 (1974).
———, and R. B. Bird, "Squeezing Flow Between Parallel Disks: I. Theoretical Analysis," *ibid.*, 336 (1974).
Metzner, A. B., "Extensional Primary Field Approximations for Viscoelastic Media," *Rheol. Acta.*, 10, 434 (1971).
Na, T. Y., "The Non-Newtonian Squeeze Film," *J. Basic Eng., Trans. ASME*, 88, 687 (1966).
Novotny, E. J., Jr., and R. Eckert, "Direct Measurement of Hole Error For Viscoelastic Fluids in Flow Between Infinite Parallel Plates," *Trans. Soc. Rheol.*, 17, 227 (1973).
Parlato, P., M. S. thesis, Univ. Del., Newark (1969).
Riddle, M. J., C. Narvaez, and R. B. Bird, "Interactions Between Two Spheres Falling Along Their Line of Centers in a Viscoelastic Fluid," *J.N.N.F.M.*, 2, 23 (1977).
Sadd, M. H., and A. K. Stiffler, "Squeeze Film Dampers: Amplitude Effects at Low Squeeze Numbers," *J. Eng. Ind.*, 97, 1366 (1975).
Salbu, E. O. J., "Compressible Squeeze Films and Squeeze Bearings," *J. Basic Eng.*, 86, 355 (1964).
Scott, J. R., "Theory and Application of the Parallel-Plate Plastimeter," *Trans. I.R.I.*, 7, 169 (1931).
Stefan, J., "Versuche über die scheinbare Adhäsion," *Akad. Wiss. Math. Natur., Wien*, 69, Part 2, 713 (1874).
Sutterby, J. L., "Falling Sphere Viscometry: I. Wall and Inertial Corrections to Stoke's Law in Long Tubes," *Trans. Soc. Rheol.*, 17, 559 (1973).
Tanner, R. I., "Some Illustrative Problems in the Flow of Viscoelastic Non-Newtonian Lubricants," *ASLE Trans.*, 8, 179 (1965).
Turian, R. M., "Thermal Phenomena and Non-Newtonian Viscometry," Ph.D. thesis, p. 112, Univ. Wisc., Madison (1964).
Williams, G., and R. I. Tanner, "Effects of Combined Shearing and Stretching in Viscoelastic Lubrication," *J. Lub. Tech., Trans. ASME*, 92, 216 (1970).

Manuscript received June 29, 1977; revision received December 8, and accepted December 16, 1977.

Liquid Distribution in Trickle-Bed Reactors

MORDECHAY HERSKOWITZ
and
J. M. SMITH
University of California
Davis, California 95616

Part I. Flow Measurements

Radial liquid distribution was measured for concurrent downflow of air and water through beds packed with catalyst particles. The experimental results can be predicted by a theory involving two parameters, a spreading factor S and wall factor *f*. Criteria are presented for predicting operating conditions (particle size and shape and tube diameter) for which the equilibrium distribution will be uniform and packed-bed depth required to attain equilibrium liquid distribution.

SCOPE

The effect of maldistribution of liquid in trickle beds has been a worrisome and unknown factor, both from the standpoint of the performance of commercial scale reactors (Ross, 1965) and interpretation of data from laboratory reactors (Satterfield, 1975; Levec and Smith, 1976). The extensive studies of liquid distribution in countercurrent flow absorption columns, summarized by Onda et al. (1973), indicated reasonably uniform flow in the central section of the packed column but excessive flow at the wall. The significant variables were distribution of the feed liquid, tvpe and size of the packing, column diameter, gas and liquid flow rates, and some physical properties.

It is expected that the same variables would be involved in the cocurrent downflow of gas and liquid in trickle beds. However, flow rates are substantially less, and the packing units, catalyst particles, are normally smaller and of different shape.

Quantitative experimental data for trickle beds appear to be limited to the papers of Prchlik et al. (1973, 1975*a*, *b*) and Specchia (1974). Their measurements were made for the pellets 0.64 to 0.98 cm in size (shape unknown) and without gas flow. The results were correlated with a diffusion type of equation involving three adjustable parameters. Unfortunately, most of the experimental data were not published in sufficient detail to be useful for evaluation purposes.

The objective of our work was twofold. We wanted to develop a method of predicting the radial distribution applicable for the gas continuous or trickling flow regime, as characterized by Charpentier (1976). This regime includes the range of gas and liquid flow rates normally encountered in trickle-bed reactors. We also wanted to measure as carefully as possible flow distributions which would be useful for evaluating our theory and others. Accordingly, data were obtained for fourteen catalyst particles of different size (0.26 to 1.1 cm), shape (granular, spherical, cylindri-

0001-1541-78-1022-0439-$01.45.

cal), and porosity as a function of feed distribution, gas and liquid flow rates, and catalyst bed depths. Most of the measurements were for deionized water and air in two columns (4.08 and 11.4 cm I.D.). Some data also were obtained to ascertain the effect of surface tension of the liquid.

A second objective was to propose criteria for attaining uniform liquid distribution at equilibrium, that is, at a bed depth beyond which the distribution does not change, and the bed depth required to reach the equilibrium distribution.

CONCLUSIONS AND SIGNIFICANCE

The distribution of liquid was measured with annular collectors located at the bottom of the bed. Considerable difficulty was encountered in developing a collecting device and an operating procedure such that reproducible and reliable data could be obtained. A major problem was to eliminate the effect of the collecting device on the true distribution in the bed. The procedure finally established gave results that could be reproduced within 10%.

Variation of liquid and gas rates over the range of superficial velocities from 0.1 to 0.5 and 0.1 to 5.0 cm/s, respectively, did not measurably influence the liquid distribution. Particle shape and size and tube diameter affected both the equilibrium distribution and the bed depth required to reach equilibrium. For ratios of tube-to-particle diameter less than about 18, the equilibrium flow distribution was nonuniform, with enhanced flow near the tube wall and deficient flow in the central sections. However, particle size and shape also affected the distribution. Uniform equilibrium distribution was achieved at lower ratios of tube-to-particle diameter for granular particles than for spheres or cylinders. Also, equilibrium distribution was reached at lower bed depths for granular particles.

Equations are proposed for predicting the flow distribution as a function of packed-bed depth. The bed is considered as an assembly of discrete particles, with radial transfer of liquid occurring at contact points between particles. The equations include two parameters: a spreading factor S which accounts for the fraction of liquid moving in the radial direction and a wall factor f which accounts for the fraction of the flow at the wall which is directed back into the bed. The theory is based upon the same procedure as proposed by Jameson (1966) but with modifications necessary to explain experimental results. The papers by Sheridan and Donald (1959*a*, *b*) were also helpful in providing information about theoretical concepts.

The theory with realistic values of the parameters S and f gave predictions in good agreement with the experimental results for all the fourteen packing-tube combinations. Further, there were sufficient data to obtain correlations of S and f as a function of tube diameter and particle diameter and shape. With these correlations, it is possible to predict the flow distribution as a function of bed depth for a known feed distribution. The correlations are limited to air and water and to the flow rates studied. While the effects of fluid density and viscosity were not studied, the measurements for fluids of different surface tension (38 to 73 dynes/cm) indicated that the flow near the wall was reduced as the surface tension was reduced. Interestingly, the spreading factor was not affected.

Using the correlations for S and f, a criterion is proposed for particle and tube diameters required to achieve uniform distribution at equilibrium. A similar criterion is presented for the bed depth required to approach the equilibrium distribution. These criteria should be useful in designing some commercial and laboratory scale trickle-bed reactors. For example, the two criteria can be used to determine the prepacking bed depth necessary to achieve equilibrium flow in a laboratory reactor and the particle size and tube diameter necessary to ensure that this distribution is uniform.

Several prior investigations provide useful information about liquid distribution in trickle beds. Porter et al. (1968) and Satterfield and Ozel (1973) both observed for the gas continuous concurrent regime that the liquid appears to flow in rivulets from particle to particle. Our observations also suggest rivulet flow. Specchia et al. (1974) studied liquid distribution over a very wide range of flow rates in a 14.1 cm I.D. tube packed with glass beads 0.6 cm in diameter. In the trickling flow regime these authors found uniform flow at equilibrium. Since d_t/p_p was large (≈ 23), this result is expected and agrees with our conclusions.

The term wall flow W is customarily used to describe the extent of nonuniform liquid distribution near the wall. We shall also use this term, which is defined as the excess flow rate of liquid adjacent to the column wall. If the distribution is measured by collecting liquid in annular sections, and the liquid is uniformly distributed in the packing, the observed W is the difference between the actual flow rate in the outer section and the flow rate expected for uniform flow. As d_t/d_p increases, the wall flow decreases. Over the years, many suggestions have been offered for the minimum value of d_t/d_p required to eliminate wall flow. Baker et al. (1935) proposed a minimum ratio of 12, while Porter (1968) suggested 20 to 25. These proposals were based primarily on data for large, hollow particles at flow conditions corresponding to absorption column operation. Prchlik (1975*b*) observed that wall flow was less than 10% as long as $d_t/d_p > 25$. Most investigators found that W was independent of total liquid rate. However, Onda et al. (1973) analyzed Porter's data and proposed a correlation in which W is a function of F_t. We hoped in our experimental studies to cover a wide enough range of variables to provide definitive answers to these questions. It should be emphasized that our conclusions are based primarily on data for air and water at 25°C (at 1 atm pressure) and for the trickling flow regime in beds packed with particles of the size and shape used as catalysts.

EXPERIMENTAL

Apparatus

The 4.08 and 11.4 cm I.D. glass columns were equipped with a movable liquid distributor (Figures 1*a*, 1*b*) at the top of the bed and a fixed collector (Figure 1*c*) at the bottom. Bed depth was changed by adding particles and raising the dis-

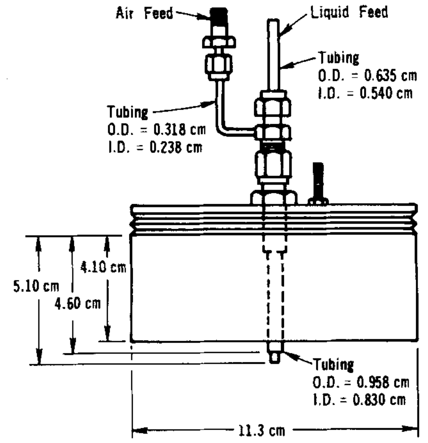

Fig. 1a. Point-source distributor.

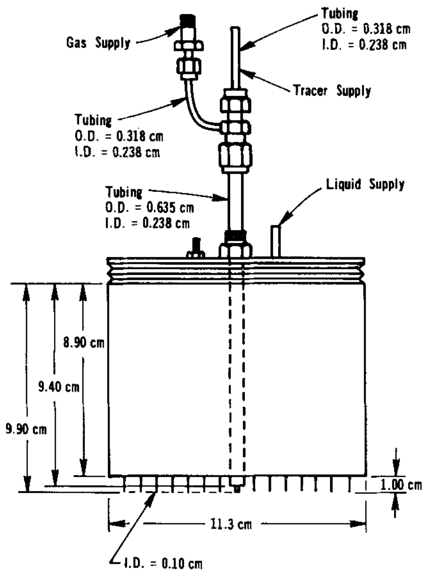

Fig. 1b. Distributor for uniform liquid feed.

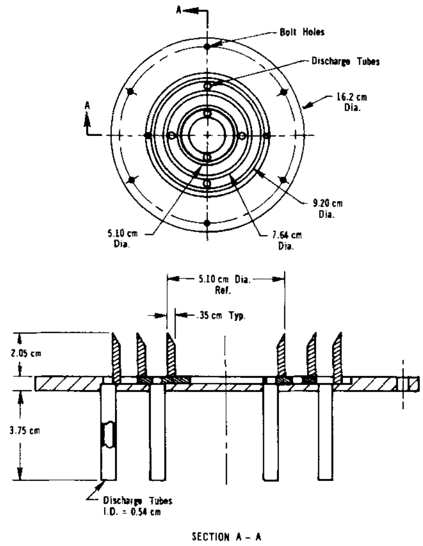

Fig. 1c. Diagram of collector B.

tributor. The liquid feed was introduced either through one small, centrally located tube (point source) or through numerous tubes (uniform distribution). In the large column, preliminary experiments with different tubes showed that the closest approach to a point source (minimum radial spread of liquid at the top of the bed) was obtained by introducing the liquid through a 0.540 cm I.D. tube whose downstream end was located 0.5 cm above the top of the bed. Actually, the approach to a point source did not determine whether the data were useful, since the distribution measured at a very low bed depth (equivalent to a few particle diameters) could be used as the known feed distribution. Feed close to a point source did give a larger change in distribution with bed depth and provided data more sensitive to the values of the parameters in the theory. For the small column, the liquid was fed through a 0.238 cm I.D. tube placed 0.3 cm above the top of the bed.

In the large column, a uniform flow of liquid was approached with a distributor containing eighty six 0.1 cm I.D. tubes arranged uniformly over the cross section of the column. The tubes were 1 cm long and located 0.5 cm above the top of the bed. Only a point source feed was used with the small column.

In the large column, the gas was introduced through an annulus (inner and outer diameters of 0.635 and 0.830 cm) surrounding the central liquid feed tube. The end of the annulus was located 1.0 cm above the top of the bed. A similar arrangement was used for the small column; the annulus for gas feed had inner and outer diameters of 0.318 and 0.540 cm and terminated 0.5 cm above the bed. The arrangement for the large column is shown in Figure 1*a*.

The key problem in designing the collector (Figure 1*c*) was to reduce the influence of the device on the flow distribution. The collectors consisted of annular acrylic plastic rings (in the small column, stainless steel rings were used) dividing the cross section of the column into three (for the small column), four, or six sections. The dimensions of these three collectors are given in Table 1, and Figure 1*c* shows collector B with four radial sections. The upper edge of the rings was beveled to a fine line in order to minimize the metal area at the top of the collector and to reduce the disturbance to the flow distribution caused by the collector rings. At first, the bed of catalyst particles was supported by a wire mesh screen and the collector located at a distance below the screen. Regardless of the screen mesh size and distance between collector and screen, the liquid migrated radially on the screen, giving unacceptable data. Ultimately, it was found that reliable data could be obtained by making the rings about 2 cm long and supporting the bed by the bottom plate of the collector (Figure 1*c*). Thus, each annular section was filled to a height of 2 cm with catalyst particles. The particles were necessary in order to prevent overflow of liquid from one annular section to an adjacent section. Preliminary measurements made by introducing liquid directly into the sections filled with particles showed no overflow over the range of gas and liquid rates studied. The dimensions of the sections were designed so that in most cases the particles were small enough to fit into the annular spaces. In those few instances where the particles were too large, the sections were filled with the same type of catalyst as used in the bed proper, but of smaller diameter.

Each annular space contained two discharge tubes located at diametrically opposite holes in the bottom plate. The use of two tubes reduced the pressure drop between the sections at the top of the collector rings and in this way reduced fluctuations in flow distribution with time. Gas and liquid were discharged through the same stainless steel tubes, which were 0.540 cm I.D. and extended 2.5 cm below the bottom plate.

Procedure

The method of packing the column affected the reproducibility of the data. The procedure that gave the most reproducible results consisted of first filling the collector sections with water and then adding particles. Next, the column was filled with water and particles added slowly, vibrating the column at frequent intervals during the process.

A run was started with the column filled with liquid so as to avoid gas bubbles. After liquid and gas flows were adjusted to the desired values, excess liquid quickly drained from the col-

Table 1. Dimensions of Collectors

Collector A (for 4.08 cm column)

	Sec. I (center)	Sec. II	Sec. III (wall)
OD, cm	2.20	3.30	4.08
ID, cm	0	2.20	3.30
% of total area	29.0	36.3	34.7

Collector B (for 11.4 cm column)

	Sec. I (center)	II	III	IV (wall)
OO, cm	5.09	7.66	9.90	11.61
ID, cm	0	5.09	7.66	9.90
% of total area	19.9	25.2	30.3	24.6

Collector C (for 11.4 cm column)

	Sec. I (center)	II	III	IV	V	IV (wall)
OD, cm	2.88	5.10	6.60	8.34	9.84	11.4
ID, cm	0	2.88	5.10	6.60	8.34	9.84
% of total area	6.4	13.6	13.5	20.0	21.0	25.5

TABLE 2. RANGE OF OPERATING CONDITIONS

	4.08 cm column		11.4 cm column	
	Liquid	Gas*	Liquid	Gas
Superficial velocity, cm/s	0.15-0.5	1.0-5.0	0.1-0.4	0.1-2.0
Superficial mass velocity, kg/(m)^2(hr)	5 400-18 000	50-250	3 600-14 400	5-100
Bed depth range, cm	0-26		0-70	

* At 25°C and 1 atm.

umn, and a steady state distribution was obtained in less than 3 min. Changes in the steady state distribution with time were less than 1%. Better reproducibility was also achieved when gas flowed concurrently with the liquid than without gas flow. The range of flow rates and bed depths studied are shown in Table 2. Over this range, preliminary runs showed no measurable change in liquid distribution with gas or liquid rates. Baker et al. (1935) and Prchlik (1975*a*, *b*) also reported no effect of gas and liquid flow rates. Further, better reproducibility was obtained when the liquid rate was increased from one value to the next, rather than reduced. It appeared that the rivulets of liquid were more stable with respect to position when the liquid rate was increased. Accordingly, the final data were obtained in the following way. At a given bed depth, gas and liquid rates were adjusted to their lowest values. Then, a series of distributions was measured by collecting liquid from each section at four or five levels of increasing liquid rates. This completed one run. The procedure was repeated starting at successively higher gas flow rates until four or five runs were made at each bed depth. The twenty to twenty five sets of distributions were then averaged arithmetically.

By this operating procedure, the deviation of the individual distributions from each other was less than 10%.

The geometric properties of the particles are given in Table 3. Void fractions were either available from the manufacturer or measured in a Beckman helium pycnometer. The equivalent diameter of the cylindrical particles was taken as the diameter of the sphere with the outer surface area of the particle. The bed depth was evaluated as the distance from the level where the feed distribution was measured to the top of the annular rings of the collector.

The surface tension of the water was changed from 73 to 38 dynes/cm by adding a fluorosurfactant (Zonyl FSP, E.I. du Pont de Nemours and Co.) in concentrations of 0.01 and 0.05 wt %.

Visual observation of the bed during the runs indicated that the liquid flowed downward over the particles in the form of rivulets which maintained their position with time. This type of flow is the same as reported by Porter (1968) and by Satterfield and Ozel (1973). In runs in which there was significant maldistribution of liquid, it appeared that the excess wall flow was contained in a region very close to the wall; that is, the wall flow extended into the bed but a small fraction of a particle diameter.

EXPERIMENTAL RESULTS

For graphical display, the distribution was expressed as the flow rate $F_{E,k}$, measured in section k, divided by the total flow rate F_t. Illustrative results are shown in Figures 2 to 6, where the fraction of the total flow in each section is plotted vs. bed depth. The dotted lines, representing uniform flow, are equal to the cross-sectional area of a section divided by the total column area.

Figure 2 displays data for two different particle sizes in the 11.4 cm column using the four-section collector (B) and point-source feed. In the central sections (I and II), the distribution changes rapidly with bed depth at low depths. This is the region where the liquid is spreading out from the point source. The distribution changes less rapidly in section IV because little liquid has reached the wall. As the bed depth increases, the situation is reversed. For the particle-tube combinations shown in Figure 2, an equilibrium distribution is closely approached at a bed depth of 55 cm. For the smallest particle ($d_t/d_p = 18$), this equilibrium distribution is uniform, while for the larger particles ($d_t/d_p = 12$), there is excess flow in the wall section (IV) and less than uniform flow in sections II and III.

In Figure 3, the effect of feed distribution is shown for 1.11 cm activated carbon particles (granular shape) packed in the 11.4 cm column. While the equilibrium distribution is far from uniform ($d_t/d_p = 10$), the same distribution is ultimately reached regardless of feed arrangement. The data show how bed depth required to reach equilibrium flow depends on the feed distribution.

The influence of particle shape is illustrated in Figure 4, where distributions are shown for granular activated car-

TABLE 3. GEOMETRICAL PROPERTIES OF PARTICLES

	Size, cm	d_p,* cm	Shape	Particle porosity	Bed void fraction
Activated carbon†	0.236-0.279	0.258	Granular	0.62	0.40
Activated carbon†	0.236-0.470	0.352	Granular	0.62	0.40
Activated carbon†	0.630-0.800	0.715	Granular	0.62	0.40
Activated carbon†	0.800-0.950	0.875	Granular	0.62	0.40
Activated carbon†	0.950-1.27	1.11	Granular	0.62	0.40
Ceramic balls**	0.953	0.953	Spherical	0	0.40
Ceramic balls**	0.635	0.635	Spherical	0	0.40
Glass beads	0.300	0.300	Spherical	0	0.40
Ceramic cylinders**	0.635 × 0.953	0.898	Cylindrical	0	0.38
Alumina cylinders***	0.635 × 0.635	0.778	Cylindrical	0.50	0.42
Alumina cylinders***	0.476 × 0.476	0.583	Cylindrical	0.50	0.42
Alumina cylinders***	0.318 × 0.318	0.389	Cylindrical	0.50	0.42

* For granular packing, $d_p = \frac{(d_p)_{min} + (d_p)_{max}}{2}$. For cylindrical packing, $d_p = \left(\frac{d^2}{2} + dh\right)^{1/2}$, where d and h are nominal values.

† Type BPL manufactured by Pittsburgh Activated Carbon Company.

** Manufactured by Norton Company, Plastics and Synthetics Division.

*** Type T-126, Chemetron Corporation

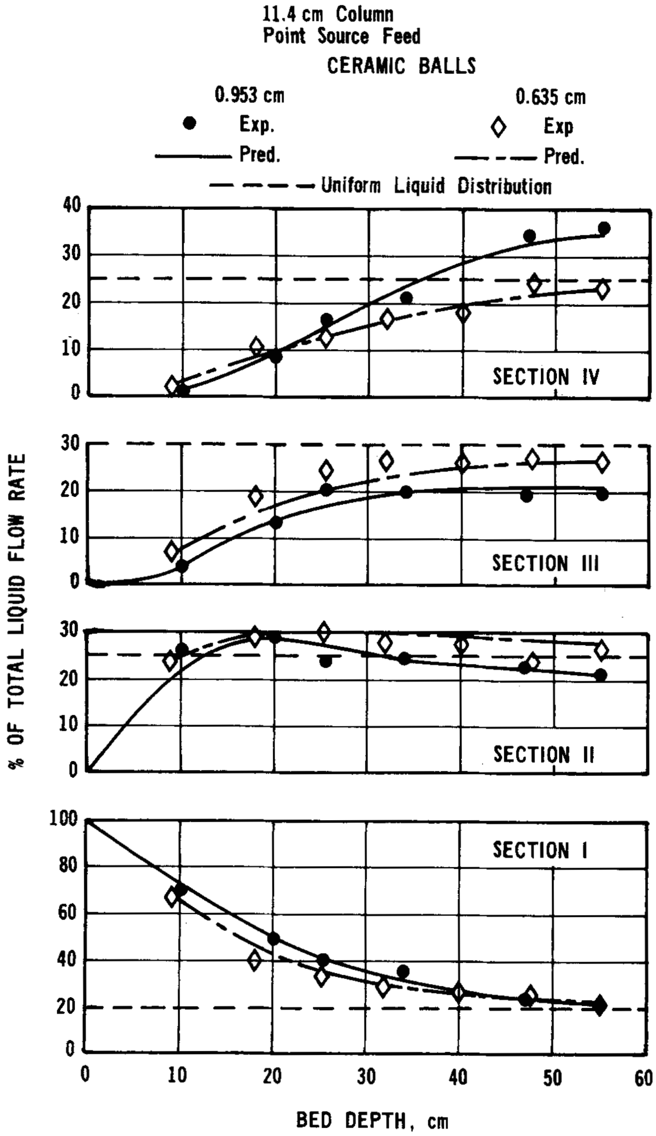

Fig. 2. Effect of particle size on liquid distribution at various bed depths.

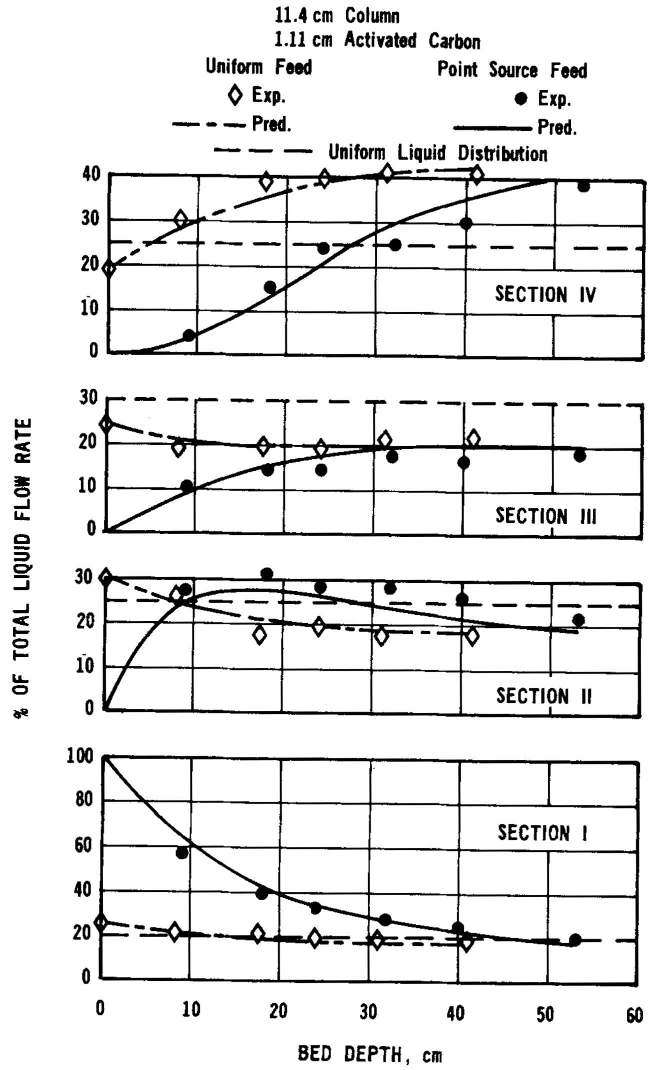

Fig. 3. Effect of feed distribution on liquid distribution vs. bed depth.

bon and alumina cylinder particles of approximately the same size. For this case, where the column-to-particle diameter ratio is about 15, the equilibrium distribution is close to uniform for the granular particles, while there is excess flow at the wall for the cylinders. Results for spherical particles were similar to those for cylinders with somewhat less wall flow. This conclusion that cylindrical and spherical particles give excess flow at the wall has been mentioned previously by Acres (1967). He postulated that in trickle-bed reactors cylindrical particles would perform relatively poorly because some of the particles would pack end-to-end and cause liquid to track through the bed, leading to nonuniform distribution. It was also suggested that spherical particles channel the liquid toward the wall.

Figure 5 is designed to show the effect of column diameter. Experimental data are plotted for activated carbon particles packed in the small, 4.08 cm column. The ratio d_t/d_p is 11.6, and the equilibrium distribution is nonuniform. Comparable experimental data for the large column cannot be shown because the collectors had a different number of sections. However, the effect of column diameter can be ascertained by using the theory described in the next section to predict what the distribution would be in a 11.4 cm column with the same 0.352 cm activated carbon particles. The value of d_t/d_p is now 32, and the equilibrium distribution would be uniform. However, a much longer bed depth is necessary to reach this equilibrium, and, as the curves show, equilibrium is not attained at the 25 cm limit of the experimental results for the small column. While the two sets of curves suggest that the liquid spreads radially at lower bed depths in the small column, the radial distance is greater in the large column. It is correct to state that the radial spread of liquid, measured in terms of fraction of the column radius, is greater in the small column.

In addition to shape, the wetting characteristics of the particles may influence the distribution. These characteristics are affected by the physical properties of the liquid, column wall, and particle. As mentioned, the effect of one such property, surface tension of the liquid, was investigated. Experiments with both cylindrical and spherical particles demonstrated that lowering the surface tension from 73 to 38 dynes/cm reduced the wall flow. This is illustrated in Figure 6 for ceramic particles at conditions such that the equilibrium distribution with deionized water is nonuniform. Comparison of the two curves in sections I and II shows that the radial spreading of the liquid is essentially unaffected by the change in surface tension. However, the wall flow, which becomes apparent in section IV as the bed depth increases, is so reduced that a uniform distribution is attained at equilibrium. This occurs even though d_t/d_p is but 12. Further investigations of the effects of such properties as surface tension, viscosity, density, etc., for different kinds of particles could lead to a

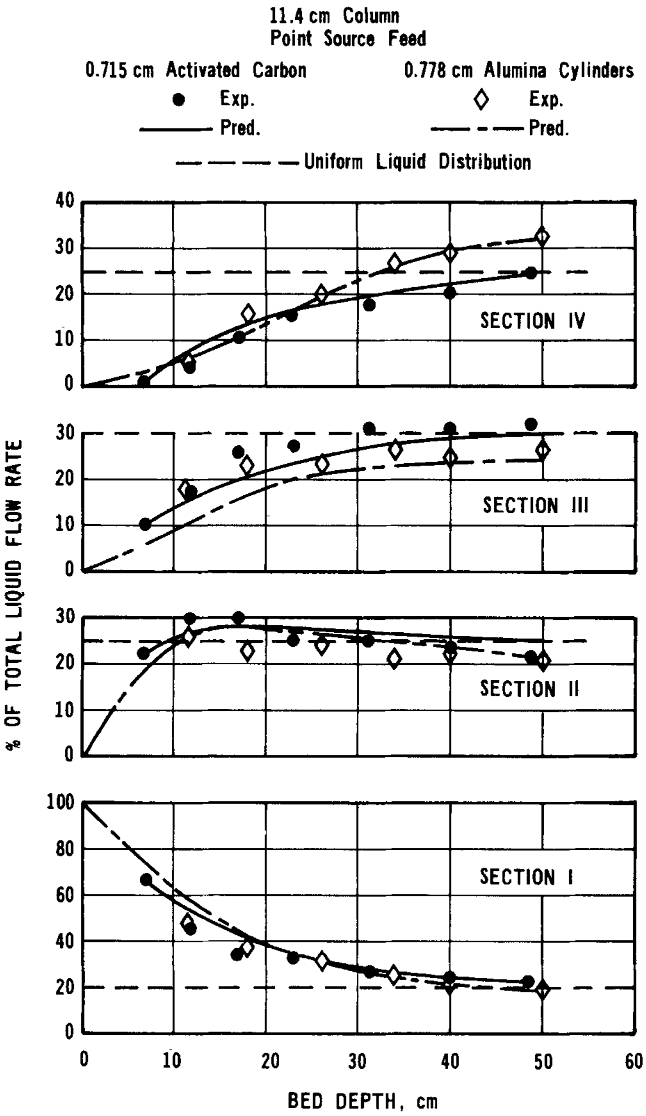

Fig. 4. Effect of particle shape on liquid distribution.

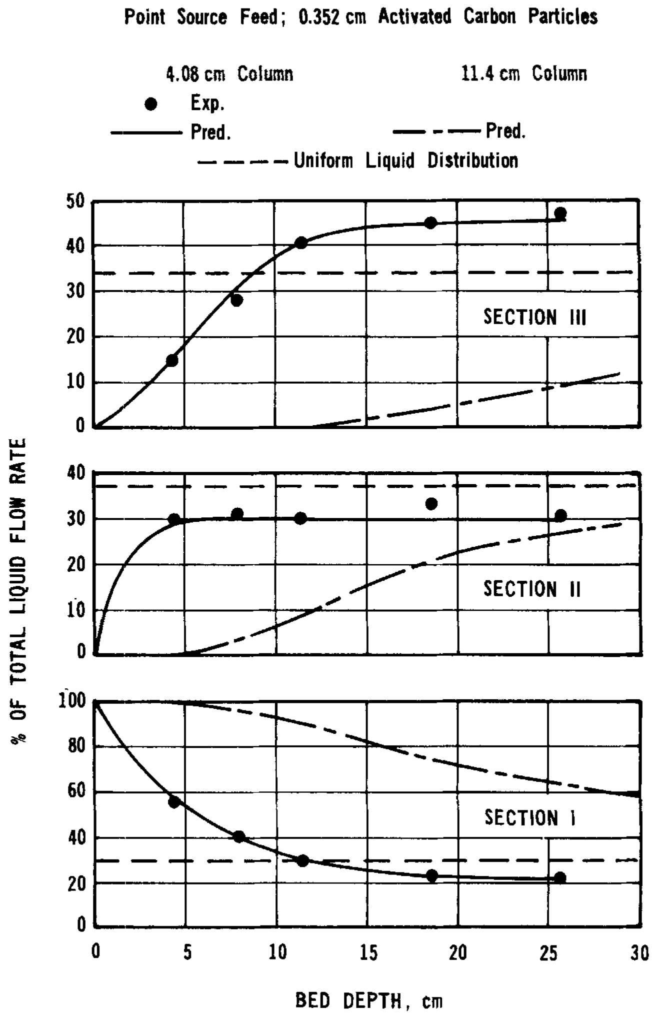

Fig. 5. Effect of column diameter on liquid distribution.

more complete understanding of the distribution phenomena.

THEORY

A model based upon the work of Jameson (1966) is used to derive predictive equations for the flow distribution. The major differences between our model and that of Jameson are in the method of evaluating the number of contact points (defined later) within the bed and in the consideration of flow at the wall. These changes lead to resultant expressions different from those of Jameson. Also, the equations presented here are capable of predicting a uniform distribution at equilibrium, as found experimentally at some conditions. The bed is regarded as an assembly of discrete spherical particles through which the liquid flows in rivulets, while the gas phase is continuous. The radius of the column and the catalyst bed depth are assumed to be divisible into an integral number of particles m and n as illustrated in Figure 7a. Thus, $R_o = m\, d_p$ and $L = n\, d_p$. The radial distance R from the center of the column is measured in terms of a dimensionless radial position $r = R/d_p$. Each horizontal layer of particles of thickness d_p is divided into m concentric, annular rings, and each ring is identified by its radial position i and bed depth j, where i and j represent integral numbers of particles. The ring (i, j) is illustrated in Figure 7b. The dimensionless distance from the center of the column to the midpoint of the (i, j) ring is $r_i = i - 0.5$. If we assume that the particles are in contact with each other (Figure 7b), the number of particles in the (i, j) ring is approximately equal to $2\pi r_i$.

Radial transfer is supposed to occur by movement of liquid from one annular ring to the next ring by flow to and mixing at contact points between rings, that is, at the points where particles in adjacent rings are in contact with each other. Three such contact points are identified in Figure 7b. This assumption seems plausible, since the liquid flows over the particles. Annular symmetry is also postulated so that flow from particle to particle in the same annular ring need not be considered.

The number of contact points between annular rings (i, j) and $(i + 1, j)$ is equal to the average number of particles in the two rings. Since the number of particles in the (i, j) and $(i + 1, j)$ rings are $2\pi(r_i d_p)/d_p$ and $2\pi(r_{i+1} d_p)/d_p$, the average number of contact points is $\pi(r_i + r_{i+1})$. As $\pi r_{i+1} = r_i + 1$, this may be written $\pi(2r_i + 1)$. Similarly, between rings (i, j) and $(i - 1, j)$ the number of contact points is $\pi(2r_i - 1)$. Hence, the total contact points in both radial directions from ring (i, j) is the sum $4\pi r_i$.

The liquid flowing in annular ring (i, j) can move radially to ring $((i + 1, j)$ or $(i - 1, j)$ via contact points, or it can flow downwards to ring $(i, j + 1)$, bypassing the contact points as shown in Figure 8. Let the fraction of the flow that goes to the contact points be S, the spreading factor. Then, if the total flow in ring (i, j) is $F_{i,j}$, the flow that bypasses the contact points will be $(1 - S)F_{i,j}$.

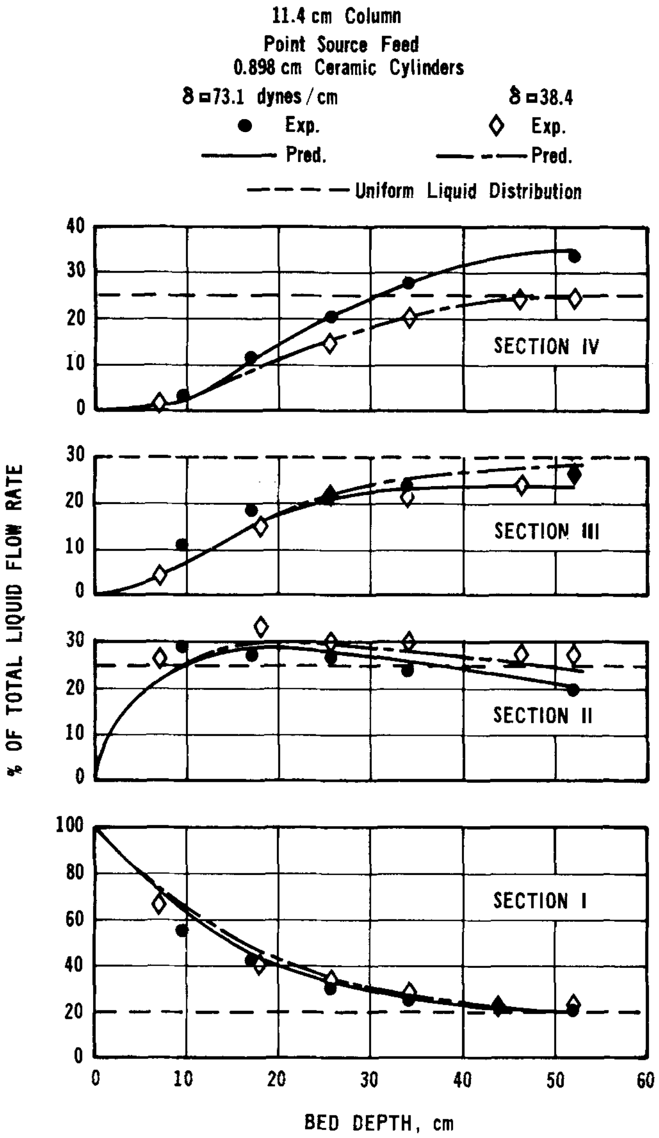

Fig. 6. Effect of surface tension on liquid distribution.

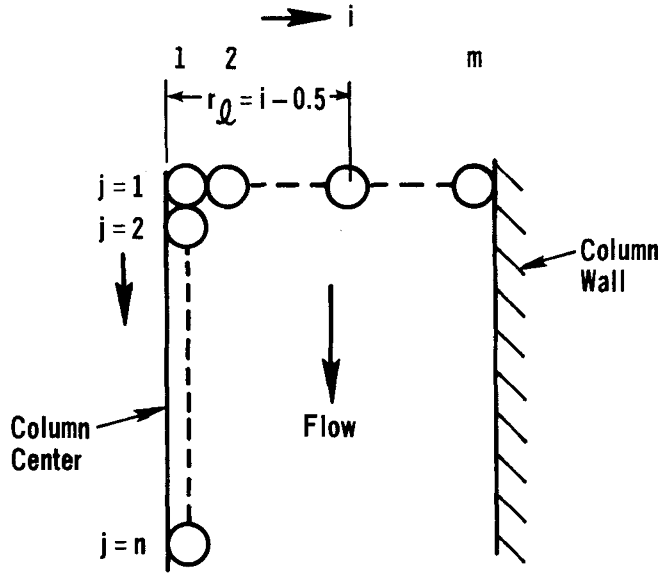

Fig. 7a. Notation for flow model (side view).

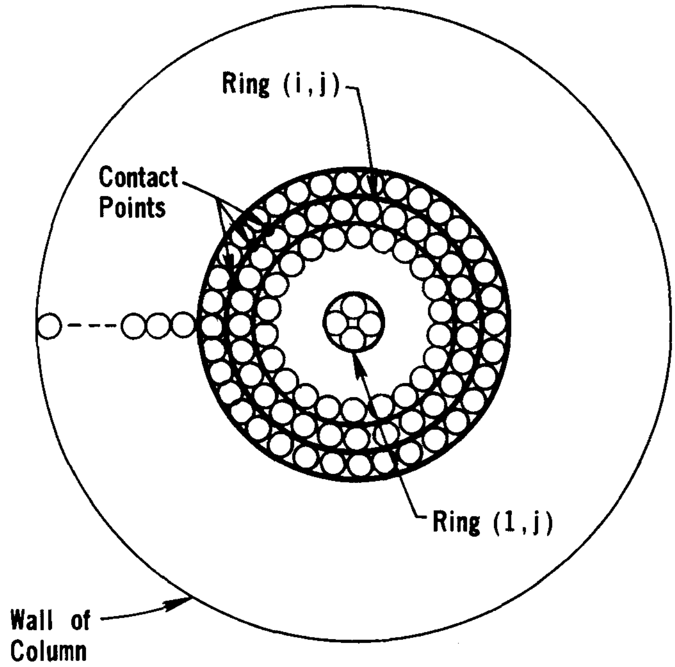

Fig. 7b. Notation for flow model (top view).

In view of the angular symmetry assumption, the remaining flow will be equally distributed among the contact points associated with ring (i, j). The flow to contact points between rings (i, j) and $(i + 1, j)$ will be $SF_{i,j}[(2r_i + 1)/4r_i]$, since the quantity in brackets is the fraction of the total contact points that connect rings (i, j) and $(i + 1, j)$. Similarly, the flow to contact points between rings (i, j) and $(i - 1, j)$ is $SF_{i,j}[(2r_i - 1)/4r_i]$. The flow reaching the contact points from rings (i, j) will be mixed at these contact points with flow from rings $(i - 1, j)$ and $(i + 1, j)$. The flow leaving the contact points is assumed to divide into two equal streams going to adjacent annular rings. For example, the flow from the contact points between rings $(i - 1, j)$ and (i, j) divides equally into streams flowing into rings $(i - 1, j + 1)$ and $(i, j + 1)$. This process of radial flow followed by downward flow via the contact points is repeated through the bed until the wall is reached. Such a flow network is illustrated in Figure 8 for rings at the j and $(j + 1)$ bed depths. By summing the three streams entering the ring $(i, j + 1)$ (two streams from the adjacent contact points and the bypass stream), an expression can be obtained for the flow at the $j + 1$ bed depth, in terms of the flow at the j level. Reference to Figure 8 shows that this equation is

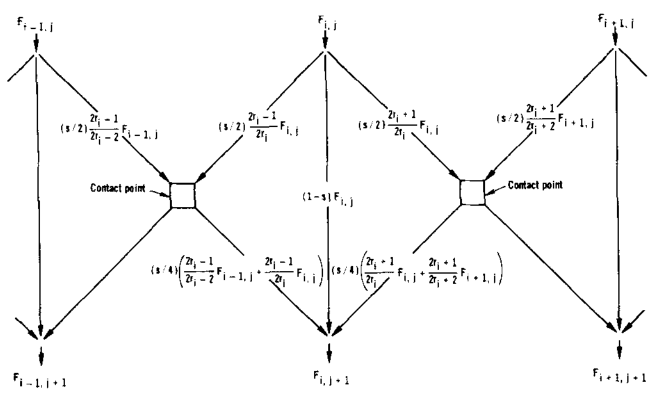

Fig. 8. Flow network in bed.

$$F_{i,j+1} = \frac{S}{4}\left(\frac{2r_i - 1}{2r_i - 2} F_{i-1,j} + \frac{2r_i - 1}{2r_i} F_{i,j}\right) + \frac{S}{4}\left(\frac{2r_i + 1}{2r_i} F_{i,j} + \frac{2r_i + 1}{2r_i + 2} F_{i+1,j}\right) + (1 - S)F_{i,j} \tag{1}$$

Equation (1) may be simplified to

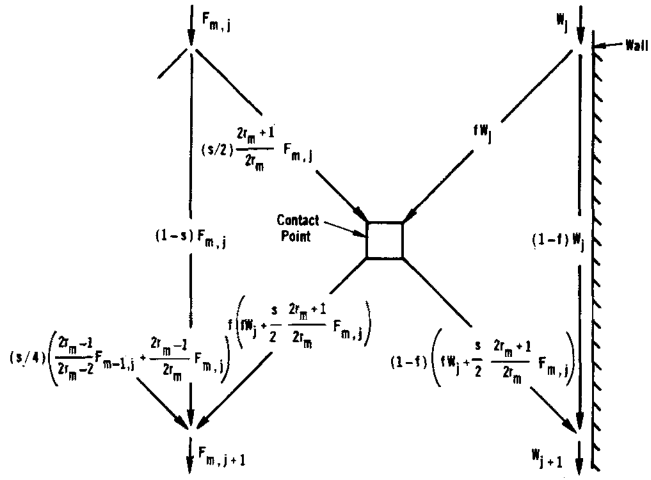

Fig. 9. Flow network near column wall.

$$F_{i,j+1} = \left(1-\frac{S}{2}\right)F_{i,j} + \frac{S}{4}\left(\frac{2r_i-1}{2r_i-2}F_{i-1,j} + \frac{2r_i+1}{2r_i+2}F_{i+1,j}\right) \qquad (2)$$

(for $j = 1$ to n and $i = 2$ to $m-1$)

For the annular ring $(1, j)$ at the center, Equation (2) is not applicable because there are contact points only on the outer side of the ring, that is, between rings $(1, j)$ and $(2, j)$. A similar summation of flows gives for $F_{1,j+1}$

$$F_{1,j+1} = \left(1-\frac{S}{8}\,\frac{2r_i+1}{r_i}\right)F_{1,j} + \frac{S}{8}\left(\frac{2r_i+1}{r_i+1}\right)F_{2,j} \qquad (3)$$

If we assume that the spreading factor S is constant, Equations (2) and (3) can be used to predict the flow distribution at any depth within the bed from a known feed distribution $F_{i,1}$.

Special equations are necessary to describe conditions in the annular ring (m, j) adjacent to the wall and at the wall. As indicated in Figure 9, the theory allows for a flow of liquid W_j in the region adjacent to the wall. This flow, as noted previously, is the excess above that expected for uniform distribution of liquid over the column cross section. For a point feed source, W can be measured experimentally only after the equilibrium distribution is attained. The wall flow is not isolated from the bed but can be increased by flow from the adjacent contact point (between wall and particle) and decreased by radial flow from the wall to the contact point. A parameter f, assumed to be constant with bed depth, is introduced to express the fraction of the wall flow that goes to a contact point. The remaining wall flow $(1-f)\,W_j$ moves downward along the wall to the next bed depth $j+1$, bypassing the contact point. Flow from the contact point to the $j+1$ bed depth is assumed to divide into two nonequal streams, the fraction f going to the annular ring $(m, j+1)$ and the fraction $1-f$ returning to the wall. This assumption allows for the possibility of an equilibrium distribution that is uniform, in agreement with the experimental results for some combinations of column and particles. Uniform flow will occur when $f = 1$, for then the wall flow will be zero.

With this flow network near the wall, there will be three streams entering annular ring $(m, j+1)$: one from annular ring $(m-1, j)$, a second from the contact points between ring (m, j) and the wall, and the bypass stream. A sum of these streams gives $F_{m,j+1}$. As indicated in Figure 9, the sum is

$$F_{m,j+1} = f\left(fW_j + \frac{S}{2}\,\frac{2r_m+1}{2r_m}F_{m,j}\right) + \frac{S}{4}\left(\frac{2r_m-1}{2r_m-2}F_{m-1,j} + \frac{2r_m-1}{2r_m}F_{m,j}\right) + (1-S)F_{m,j}$$

or, simplifying

$$F_{m,j+1} = f^2W_j + \left[\frac{Sf}{2}\left(1+\frac{1}{2r_m}\right) + \frac{S}{4}\left(1-\frac{1}{2r_m}\right) + 1 - S\right]F_{m,j} + \frac{S}{4}\,\frac{2r_m-1}{2r_m-2}F_{m-1,j} \qquad (4)$$

The wall flow at $(j+1)$ bed depth will be the sum of two streams, one from the contact points and the bypass stream. This sum will be

$$W_{j+1} = (1-f)\left[fW_j + \left(\frac{S}{2}\right)\frac{2r_m+1}{2r_m}F_{m,j}\right](1-f)W_j$$

or

$$W_{j+1} = (1-f)\left[(1+f)W_j + \left(\frac{S}{2}\right)\frac{2r_m+1}{2r_m}F_{m,j}\right] \qquad (5)$$

Equations (4) and (5) can be used to predict the flow, at successively larger bed depths, in the annular ring next to the wall and at the wall, respectively.

In addition to the prior equations, an expression can be developed for the wall flow at equilibrium in terms of parameters S and f. For values of j such that equilibrium is reached, $F_{i,j} = F_{i,j+1} = F_{i,\infty}$. Since the number of particles in annular ring (i, j) has already been shown to be $2\pi r_i$, the flow rate $(F_p)_{i,\infty}$ per particle at equilibrium will be

$$(F_p)_{i,\infty} = \frac{F_{i,\infty}}{2\pi r_i} \qquad (6)$$

While this equation suggests that $(F_p)_{i,\infty}$ can vary with radial position, we can show that it is independent of i. This is done by substituting, for $F_{1,j+1}$, $F_{1,j}$, and $F_{2,j}$ in Equation (3), expressions for the equivalent quantities $F_{1,\infty}$ and $F_{2,\infty}$ obtained from Equation (6) for $i = 1$ and $i = 2$. This yields $(F_p)_{1,\infty} = (F_p)_{2,\infty}$. Proceeding in a similar manner in Equation (2) for $i = 2$, one obtains $(F_p)_{3,\infty} = (F_p)_{2,\infty}$. This process can be continued for $i = 3$. Hence, $(F_p)_{i,\infty}$ is a constant $(F_p)_\infty$. This means that at equilibrium the flow per particle will be the same anywhere in the bed, although there may be an additional flow at the wall. This conclusion is in agreement with the experimental results. For example, equilibrium is closely approached at the maximum bed depths in Figures 2 and 3. If the equilibrium value for the fraction of the total flow in a section is divided by the area of that section, a quantity proportional to the flow per particle is obtained. Doing this for all the sections, except that at the wall, gives approximately the same result.

The total flow rate F_t in the column may be expressed as the wall flow plus the flow in the bed; that is

$$F_t = W_\infty + P(F_p)_\infty \qquad (7)$$

where P is the total number of particles in one horizontal layer of the bed. Since the number of particles in annular ring (i, j) is $2\pi r_i$

$$P = \sum_{i=1}^{m} 2\pi r_i = 2\pi \sum_{i=1}^{m} r_i$$

Table 4. Parameter Values from Experimental Flow Data

Particle	d_p, cm	d_t, cm	d_t/d_p	S	f	f^*	Collector	
Activated C	0.258	4.08	15.8	1.00	0.85	0.85	A	
Activated C	0.352	4.08	11.6	1.00	0.57	0.57	A	
Activated C	0.352	11.4	32.4	1.00	1.00	—	C	Point source and uniform distribution
Activated C	0.715	11.4	15.9	1.00	1.00	—	B	
Activated C	0.875	11.4	13.0	0.80	0.62	0.62	B	
Activated C	1.11	11.4	10.3	0.57	0.40	0.40	B	Point source and uniform distribution
Ceramic balls	0.953	11.4	12	0.55	0.40	0.40	B	
Ceramic balls	0.635	11.4	18	0.90	1.00	—	B	
Glass beads	0.300	4.08	13.6	1.00	0.62	0.62	A	
Glass beads	0.300	11.4	38	1.00	1.00	—	C	
Ceramic cyl.	0.898	11.4	12.7	0.70	0.48	0.48	B	
Alumina cyl.	0.778	11.4	14.7	0.80	0.53	0.53	B	
Alumina cyl.	0.583	11.4	19.6	1.00	1.00	—	B	
Alumina cyl.	0.389	11.4	29.3	1.00	1.00	—	C	Point source and uniform distribution

* Calculated from Equation (10).

The summation is that of an arithmetic series which is given (Selby, 1971) as $(r_1 + r_m)m/2$. Hence

$$P = 2\pi \frac{(r_1 + r_m)m}{2} = \pi[1 - 0.5 + m - 0.5]m$$

$$P = \pi\, m^2 = \pi(r_m + 0.5)^2 \tag{8}$$

With this result, Equation (7) becomes

$$F_t = W_\infty + \pi(r_m + 0.5)^2 (F_p)_\infty \tag{9}$$

At equilibrium, $W_j = W_{j+1} = W_\infty$. Replacing W_{j+1} and W_j with W_∞ in Equation (5) gives an expression for $F_{m,j}$ in terms of W_∞. Since $F_{m,j} = F_{m,\infty}$ and $F_{m,\infty} = 2\pi r_m (F_p)_\infty$ from Equation (6) at equilibrium, we can obtain $(F_p)_\infty$ in terms of W_∞. Finally, if this expression for $(F_p)_\infty$ is substituted in Equation (9), the result is

$$\frac{W_\infty}{F_T} = \left[1 + \frac{f^2 (r_m + 0.5)}{S(1-f)}\right]^{-1} = \left[1 + \frac{f^2 R_o}{d_p S(1-f)}\right]^{-1} \tag{10}$$

Equation (10), applicable when the bed depth is sufficient to reach equilibrium, provides a means of predicting the wall flow W_∞ in terms of the parameters S and f and the geometry of the bed. In the next section we use Equation (10) in the reverse way to provide an independent confirmation of f from the known W_∞.

DATA ANALYSIS

The flow measurements in the various sections of the collectors for the feed condition and at a given bed depth were used to calculate the parameters S and f. Each section contained a specific number of annular rings. Hence, the measured flow in that section is equal to the sum of the flows in the annular rings of the section. Equations (2), (3), and (4) provide expressions for calculating $F_{i,j+1}$ from $F_{i,j}$ for the first ring, intermediate rings, and the ring at the wall in terms of S and f. Equation (5) gives the wall flow that must be added to the flow in the rings in the last section to obtain the total flow in that section. The procedure was to assume values for S and f and start the calculations at the feed $j = 1$. With Equations (2) to (5), the flow in each of the collectors at $j = 2$ can be evaluated. The procedure is repeated until the bed depth is reached for which the flow rates were measured. Comparison of the predicted and experimental flow rates in each section determines the suitability of the assumed values of S and f. This comparison can be made at each bed depth for which experimental measurements are available. The chosen values for S and f were established by minimizing the squares of the deviations between experimental $F_{E,k}$ and predicted $F_{C,k}$ flow rates for the various sections k of the collector. That is the quantity b was minimized, where

$$b = \sum_k \frac{[F_{E,k} - F_{C,k}]^2}{F_{C,k}} \tag{11}$$

Since the data with a point feed showed the largest change in distribution, these runs were used to calculate S and f. At short bed depths, the liquid does not reach the wall ($W_j = 0$) so that only S is involved in the calculations. At large bed depths, where the distribution in the bed approaches equilibrium, only the wall factor is important. Hence, the optimization process for S and f was simple and did not require a special technique. As S and f should be independent of bed depth, data at intermediate depths could be used to make minor improvements in the parameter values. Equation (10), which could be used in those cases where equilibrium was obtained, provided a further test of S and f.

Table 4 shows S and f determined in this way for the fourteen column-particle combinations. The quantity f^* represents the value of f calculated from Equation (10) by supposing that S is correct. The predicted flow rates $F_{C,k}/F_t$ for each section, using the S and f values in Table 4, are shown as dotted lines in Figures 2 to 5. The agreement between experimental and predicted results suggests that the flow model is satisfactory for correlating flow distributions in trickle beds over the range of conditions investigated.

The spreading factor is a strong function of particle diameter and also depends upon particle shape. Figure 10 shows the results in Table 4 plotted in terms of those properties. Granular particles have larger S values, which means that the liquid spreads more radially at a given bed depth than spherical or cylindrical particles. Equilibrium distribution is attained at a lower bed depth for the granular material. For the air-water system, our data indicate S has its maximum value of 1.0 for all particles smaller than about 0.6 cm.

The wall factor can be expressed as a function of d_t/d_p

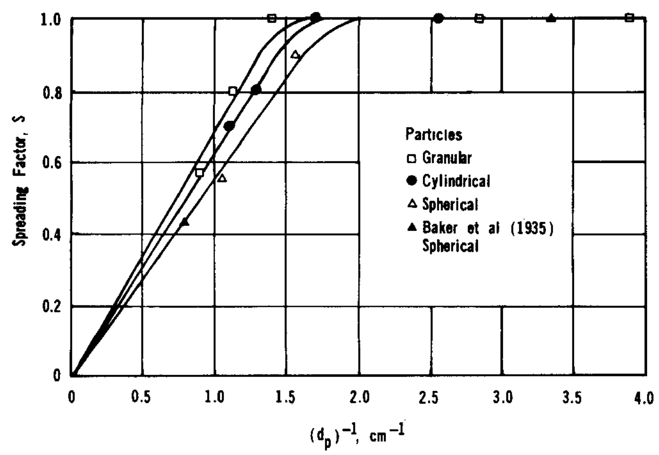

Fig. 10. Spreading factor correlation.

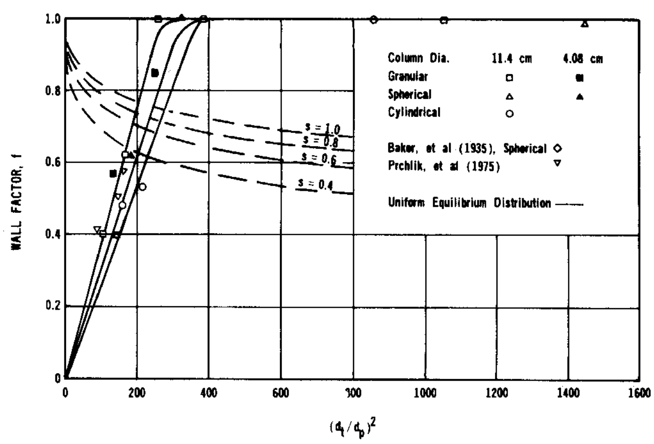

Fig. 11. Wall factor correlation.

and the type of particle, as shown in Figure 11. Separate effects of column diameter and particle size may exist but were too small to be evident from our experiments. For $f = 1$, uniform flow distribution is obtained. Figure 11 indicates that this condition is reached at $d_t/d_p = 18$ for cylinders and at a somewhat lower ratio for spheres and granular particles. At lower ratios, the extent of wall flow is sensitive to both the ratio and particle shape.

Little information is available in the literature with which to compare our results, since most distribution measurements have been made for large, hollow particles in countercurrent flow (absorption column operation). Baker et al. (1935) obtained distributions in a 15.2 cm column packed with 1.27 cm spheres. Values of S and f calculated from his data, which correspond to nonuniform equilibrium distribution, are also included in Figures 10 and 11. Prchlik and co-workers (1975*a*, *b*) measured wall flow at equilibrium in an 8.4 cm diameter column packed with 0.64, 0.69, and 0.88 cm pellets. Sufficient information was not available to evaluate S. However, we can make partial use of their data by using spreading factors estimated from Figure 10 and by assuming that the particles were granular in shape. With such values of S and the experimental wall flow rates W_∞, the wall factor was calculated from Equation (10). The results, shown in Figure 11, agree well with the curve for granular particles.

The correlations in Figures 10 and 11 seem well enough established to be useful for predicting S and f and, with Equations (2) to (5), the flow distribution in trickle beds as a function of bed depth. However, the effects of physical properties of the fluids were not studied, so that the results are limited to systems with properties similar to those of air and water. Surface tension of the liquid might be expected to affect the results. Distributions were measured with water to which surfactant had been added to reduce the surface tension to 52 and 38.4 dynes/cm. The density and viscosity remained essentially the same, but other properties, such as elasticity, could also have changed. The values of S and f calculated from these data are given in Table 5 and are plotted vs. $(\delta)^{-1}$ in Figure 12. For both the cylindrical and spherical particles, the spreading factor was unaffected by reducing the surface tension, but the wall factor was about inversely proportional to δ (Figure 12). This means that wall flow was reduced by reducing the surface tension. In fact, reducing δ from 73 to 38 dynes/cm changed the equilibrium dis-

TABLE 5. EFFECT OF SURFACE TENSION OF LIQUID

Particles	d_p, cm	Surface tension, dynes/cm	S	f
Ceramic balls	0.953	73.1	0.55	0.40
Ceramic balls	0.953	52	0.55	0.60
Ceramic balls	0.953	38.4	0.55	0.80
Ceramic cylinders	0.898	73.1	0.70	0.48
Ceramic cylinders	0.898	52	0.65	0.60
Ceramic cylinders	0.898	38.4	0.70	0.85

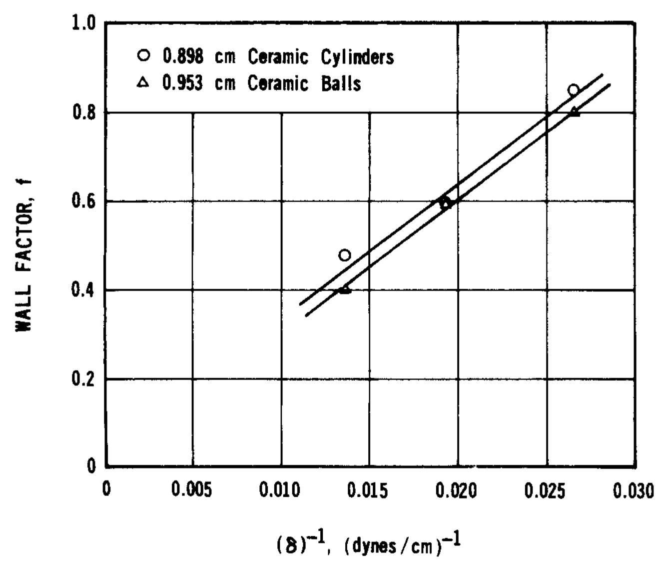

Fig. 12. Effect of surface tension on wall factor, f.

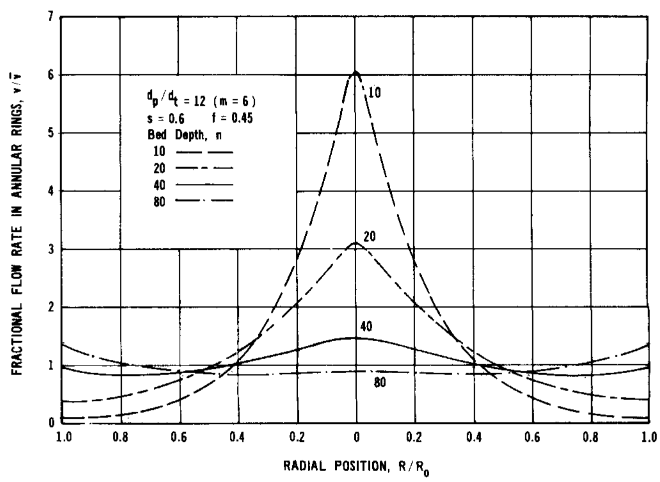

Fig. 13. Predicted liquid distribution for point source feed.

Table 6. Minimum Bed Depth for Equilibrium Flow Distribution

	$d_p/d_t = 8$; $f = 0.15$			$d_p/d_t = 8$; $f = 0.25$			$d_p/d_t = 10$; $f = 0.25$			$d_p/d_t = 10$; $f = 0.40$			$d_p/d_t = 12$; $f = 0.40$		
S	n_p	n_u	W_n/F_t	n_p	n_u	W_n/F_t	n_p	n_u	W_n/F_t	n_p	n_u	W_n/F_t	n_p	n_u	W_n/F_t
1.0	70	46	0.90	55	42	0.74	74	56	0.70	60	44	0.42	93	53	0.38
0.8	80	54	0.88	62	48	0.70	82	63	0.65	69	48	0.37	106	57	0.33
0.6	96	65	0.84	72	57	0.63	98	73	0.58	82	53	0.31	126	62	0.27
0.4	119	83	0.78	93	69	0.54	126	86	0.48	106	58	0.23	151	66	0.19

	$d_p/d_t = 12$; $f = 0.60$			$d_p/d_t = 14$; $f = 0.55$			$d_p/d_t = 14$; $f = 0.75$			$d_p/d_t = 16$; $f = 0.7$			$d_p/d_t = 16$; $f = 1$		$d_p/d_t = 18$; $f = 1$		$d_p/d_t = 20$; $f = 1$	
S	n_p	n_u	W_n/F_t	n_p	n_u	W_n/F_t	n_p	n_u	W_n/F_t	n_p	n_u	W_n/F_t	n_p	W_n/F_t	n_p	W_n/F_t	n_p	W_n/F_t
1.0	77	35	0.16	83	42	0.17	75	42	0.059	94	56	0.070	105	~ 0	124	~ 0	144	~ 0
0.8	88	36	0.13	97	43	0.14	89	42	0.048	111	63	0.056	136	~ 0	148	~ 0	171	~ 0
0.6	105	37	0.098	118	43	0.11	111	42	0.036	137	73	0.043	157	~ 0	184	~ 0	213	~ 0
0.4	136	35	0.067	157	42	0.076	150	42	0.024	184	88	0.028	214	~ 0	250	~ 0	288	~ 0

tribution from distinctly nonuniform to nearly uniform. It would be helpful to have additional data on the effects of physical properties so that the correlations in Figures 10 and 11 could be modified to be useful for other fluids.

Figure 13 illustrates expected liquid distribution as a function of bed depth as calculated for 1.0 cm spherical particles in a column 12 cm in diameter. From Figures 10 and 11, $S = 0.6$ and $f = 0.45$. Then, the flow rate in each of the six angular rings was calculated from Equations (2) to (5), adding the wall flow to the $m = 6$ ring. A point-source feed was used. The ordinate in Figure 13 is the flow rate v per unit column area divided by the average flow rate $\overline{v}$ per unit area over the whole column. The values of v were obtained by dividing the flow rate in each ring by the area of the ring.

CRITERIA

Suppose, for an equilibrium wall flow W_∞ of 5% or less of the total liquid rate, that the distribution can be regarded as uniform. If we substitute $W_\infty/F_t = 0.05$ in Equation (10), f may be represented as a function of d_t/d_p and S. This relationship is indicated by the dashed curves superimposed upon the solid curves in Figure 11. In practice, the column diameter and particle diameter and shape would be known. Thus, the spreading factor could be obtained from Figure 10. Then, from d_t/d_p and the particle shape, f could be ascertained from one of the solid curves in Figure 11. If this f is greater than that given by the intersection of the appropriate solid and dashed curves, the equilibrium flow distribution will be uniform.

The approach to an equilibrium flow distribution can be defined in terms of the change in flow rate, in the annular rings, with bed depth. Suppose we assume that equilibrium is attained if this change is 5% or less summed over all rings and including wall flow. Then, the requirement may be written

$$\sum_{i=1}^{m} \left(\frac{F_{i,\infty} - F_{i,n}}{F_{i,\infty}} \right) + \frac{W_\infty - W_n}{W_\infty} \leq 0.05 \qquad (12)$$

Here, $F_{i,\infty}$ is the flow rate at equilibrium, and $F_{i,n}$ is the flow rate at a bed depth $L = n\, d_p$. The n value that satisfies Equation (12) can be found for a given S and f by calculating $F_{i,\infty}$, W_∞, and $F_{i,n}$ for various n from Equations (2) to (5). The results depend upon the feed distribution. Values of n so calculated are given in Table 6 for point-source feed n_p and uniform feed n_u. In order to use this table to predict the bed depth necessary to reach the equilibrium distribution, S and f would first be evaluated from Figures 10 and 11 from d_p, d_t, and the particle shape. Then, the appropriate $n (= L/d_p)$ value is found from the table. The columns labeled W_n/F_t give the wall flow corresponding to the n values. These wall flows, which are a measure of nonuniform distribution, are independent of the feed distribution since they are for close-to-equilibrium conditions.

ACKNOWLEDGMENT

The financial assistance of the National Science Foundation, Grant ENG 76-00153, and the Regents of the University of California are gratefully acknowledged. We also thank R. Powell for carrying out part of the experimental work. Chemetron Corporation, Pittsburgh Activated Carbon, the Norton Company, and Kaiser Chemical Company kindly provided the particles for the bed.

NOTATION

- b = deviation variable defined in Equation (11), cm^3/min
- d_p = equivalent particle diameter, cm
- d_t = I.D. of column, cm
- $F_{i,j}$ = liquid flow rate in ring (i, j), cm^3/min
- $F_{i,\infty}$ = liquid flow rate at equilibrium bed depth, cm^3/min
- $F_{E,k}$ = experimental flow rate in section k of collector, cm^3/min
- $F_{C,k}$ = predicted flow rate in section k of collector, cm^3/min
- $(F_p)_{i,\infty}$ = liquid flow rate per particle at radial position i at equilibrium, cm^3/min
- F_t = total liquid flow rate in column, cm^3/min
- f = wall factor
- h = length of cylindrical particles, cm
- i = number of particles measured radially from center of bed (Figure 7a)
- L = total catalyst bed depth, cm
- m = dimensionless radius of column, R_o/d_p
- n = total dimensionless catalyst bed depth, L/d_p
- P = number of particles in a horizontal layer of bed
- n_p = dimensionless catalyst bed depth at near equilibrium for a point-source feed
- n_u = dimensionless catalyst bed depth at near equilibrium for a uniformly distributed feed
- R = radial distance from center of column, cm
- R_o = radius of column, cm

r_i = dimensionless radius of annular ring (i), R/d_p
S = spreading factor
v = flow rate per unit of column area at any radial position, cm^3/min
$\bar{v}$ = average flow rate per unit area over entire column, cm^3/min
W = wall flow rate; W_j = wall flow rate at bed depth j; W_∞ = wall flow rate at equilibrium, cm^3/min
z = bed depth, cm
δ = surface tension, dynes/cm

Subscripts

j = dimensionless bed depth, z/d_p; identification of particle in axial direction
∞ = equilibrium
i = annular ring (i) at any bed depth
m = annular ring next to the wall

LITERATURE CITED

Acres, G. J. K., "Trickle Column Reactors. Technique for the Continuous Performance of Liquid-Phase Catalyzed Reactions," *Platinum Metals Rev.*, **11**, 86 (1967).

Baker, T., T. H. Chilton, and H. C. Vernon, "The Course of Liquid Flow in Packed Towers," *Trans. Am. Inst. Chem. Engrs.*, 31, 296 (1935).

Charpentier, J. C., "Recent Progress in Two-Phase Gas-Liquid Mass Transfer in Packed Beds," *Chem. Eng. J.*, 11, 161 (1976).

Jameson, G. J., "A Model for Liquid Distribution in Packed Columns and Trickle-Bed Reactors," *Trans. Inst. Chem. Engrs.*, **44**, T198 (1966).

Levec, J., and J. M. Smith, "Oxidation of Acetic Acid Solutions in a Trickle Bed Reactor," *AIChE J.*, **22**, 159 (1976).

Onda, K., H. Takeuchi, Y. Maeda, N. Takeuchi, "Liquid Distribution in Packed Columns," *Chem. Eng. Sci.*, **28**, 1677 (1973).

Porter, K. E., J. J. Templeman, and V. D. Barnett, "II. The Spread of Liquid over Random Packings," *Trans. Inst. Chem. Engrs.*, **46**, T74 (1968).

Porter, K. E., and J. J. Templeman, "III. Wall Flow," *ibid.*, **46**, T86 (1968).

Prchlik, J., J. Soukup, V. Zapletal, and V. Ruzicka, "Liquid Distribution in Reactors with Randomly Packed Porous Beds," *Colln. Czech. Chem. Commun. (English)*, **40**, 845 (1975*a*).

————, "Wall Flow in Trickle Bed Reactor," *ibid.*, 3145 (1975*b*).

Ross, L. D., "Performance of Trickle-Bed Reactors," *Chem. Eng. Progr.*, **61**, 77 (1965).

Satterfield, C. N., and F. Ozel, "Direct Solid-Catalyzed Reaction of a Vapor in an Apparently Completely Wetted Trickle Bed Reactor," *AIChE J.*, **19**, 1259 (1973).

Satterfield, C. N., "Trickle-Bed Reactors," *ibid.*, **21**, 209 (1975).

Selby, S. M., ed., *Standard Mathematical Tables*, 19 ed., The Chemical Rubber Co., Sandusky, Ohio (1971).

Sheridan, M. B., and M. B. Donald, "The Mechanism of Liquid Flow in Packed Columns," *Ind. Chem.*, **35**, 439 (1959*a*).

————, "The Mechanism of Liquid Flow in Packed Columns," *ibid.*, 487 (1959*b*).

Soukup, J., K. Kolomaznik, V. Ruzicka, and J. Prchlik, "Spreading Coefficient in Randomly Packed Porous Beds," *Colln. Czech. Chem. Commun. (English)*, 38, 3742 (1973).

Specchia, V., A. Rossini, and G. Baldi, "Distribution and Radial Spread of Liquid in Two-Phase Concurrent Flows in a Packed Bed," *Ing. Chim. Ital.*, **10**, 171 (1974).

Manuscript received June 17, 1977; revision received December 5, and accepted December 16, 1977.

Part II. Tracer Studies

An aqueous solution of potassium chloride tracer was introduced at a central location in the water feed to a trickle bed, and the tracer concentration was measured at various radial positions and bed depths. From the model and parameters of liquid distribution proposed in Part I, tracer concentrations can also be predicted. The predicted and experimental concentrations usually agreed within a few percent, providing an independent evaluation of the flow distribution model.

SCOPE

Liquid distribution in packed beds can be evaluated indirectly from measurements of the radial spreading of a soluble tracer. Onda et al. (1973), Specchia et al. (1974), and Stanek and Kolar (1974) have made such measurements, particularly for the kinds of large particles used in absorption columns. The radial distribution was obtained by analyzing the data with a diffusion type of equation.

The theory for liquid distribution presented in Part I can be adapted to predict tracer concentrations as a function of radial position, packed-bed depth, and feed condition. Accordingly, we have measured tracer concentrations for conditions (particle size, liquid and gas flow rates) applicable to trickle-bed reactors. These data were then compared with predicted results in order to have an independent evaluation of the theory presented in Part I.

CONCLUSIONS AND SIGNIFICANCE

The flow distribution concepts proposed in Part I can be used to predict tracer concentrations by supposing that the streams entering a contact point, between adjacent annular rings, are completely mixed and leave with a uniform concentration. Such predictions differed from measured concentrations by no more than a few percent, except for some instances for the collector at the wall. The measurements were made for granular, spherical, and cylindrical particles in both the 4.08 and 11.4 cm I.D. columns. In view of the independence of distribution on liquid flow rate found in Part I, data were obtained for